REVISTA INTERDISCIPLINAR DE PESQUISA EM ENGENHARIA

CILAMCE 2016
XXXVII IBERIAN LATIN AMERICAN CONGRESS ON COMPUTATIONAL METHODS IN ENGINEERING
BRASÍLIA - DF - BRAZIL

ELASTOPLASTIC FINITE ELEMENT ANALYSIS OF THE TEMPER ROLLING PROCESS

Yukio Shigaki - yukio@des.cefetmg.br

Jonatas Mezêncio Silva – jonatasmsm@gmail.com

Frederico Costa Magalhães – fredmag@br.inter.net

Rafael Narciso Mendes Alvarenga Romie – rafael_narciso_romie@hotmail.com

Federal Centre of Technological Education of Minas Gerais (CEFET-MG)

Amazonas avenue, 7675 - Campus II, - CEP 30510-000 - Belo Horizonte/MG, Brazil

Luciano Pessanha Moreira - luciano.moreira@metal.eeimvr.uff.br

Universidade Federal Fluminense

Trabalhadores avenue, 420, CEP 27255-125, RJ, Volta Redonda, Brazil

Abstract. *The cold temper rolling process is one of the last steps on the production of thin strips, and has many purposes. It is characterized for the low reduction applied on the strip, usually of the order of 0.5 ~5%. Temper rolling is used to improve the final flatness of the strip and its metallurgical properties, eliminate upper and lower yield stress behavior, achieve a better surface finishing and, sometimes, induce magnetic properties. The conditions in the roll bite are different from other kinds of cold rolling in reversible and tandem rolling mills. As was mentioned before, the reduction is very low, the deformation of the roll is very localized in the arc of contact area and there is considerable elastic spring back of the strip. These differences make the calculation of the rolling load very difficult. Furthermore there is lack of information of the process that show the need for a deeper research on the subject of the temper rolling process of metal strips. In this work the temper rolling process is modelled with the elastoplastic finite element method, dynamic explicit, in the plane strain state in order to a better understanding of the process. Modelling details are also given.*

Keywords: *Temper rolling, Finite element method, Flat rolling*

1 INTRODUCTION

The rolling process of strips is one of the most efficient metalforming processes, producing flat products with excellent dimensional tolerances and surface finishing at high production rates. It consists of passing through a flat strip between two rolls that reduce its thickness. The trend for more and more thinner and harder materials is a constant market requirement and rolling mills have to deal with it. In cold rolling of thin strips, the elastic deformation of the rolls takes an important role in the process, being the governing point of the whole process.

Thin cold rolled strips usually are temper rolled, as a final finishing process that improves the surface quality of the rolled material, defines its yield stress in order to avoid defects as Lüder's bands when the annealed strip is cold formed, corrects the flatness of the strip, and sometimes is used to induce magnetic properties.

In the temper rolling process the reductions are of order of 0.5% to 5%. The main objective is to apply a small plastic deformation on the strip's surface and don't affect the strip's thickness, avoiding excessive work hardening and loss of ductility, Wiklund et al., (2004). These low values for reduction makes the temper process unique, and the traditional mathematical models to calculate the rolling load and torque do not apply anymore. The artificial way of the Hitchcock's method to take into account the elastic deformation of the work rolls via a new and greater radius can't be used for temper rolling modeling, as the rolls deform far more and in a clearly noncircular shape.

For very low reductions and for thin strips, the elastic strain becomes of the order of the plastic strains, and the amount of the thickness change sometimes may be compared to the roughness of the surface, according to Pawelski (2000) in Lenard (2014).

As the reductions in the thickness are ordinarily very low, what happens in the very beginning of the plastic region of a flow curve is extremely important. Roberts (1988) and Fang et al. (2002) showed that the yield strength σ_y decreases for reductions less than 0.5%. Yet in this region, σ_y is heavily dependent on the strain rate of the uniaxial tension test. A typical flow curve for steels can be seen in Figure 1.

Several models were developed in order to calculate the flat rolling load and torque for cold rolling process. Some of them may be used with an online control system, others do not. Included in the fastest models are those based on semi-experimental studies and the slab method with Hitchcock's correction for deformed roll. More recent ones that belong to this class are those that include the "real" deformation of the rolls usually based on an influence method for the roll's deformation, that is coupled with a slab method, and considers a neutral region in the middle of the arc of contact between the work roll and the strip. These are more suited for temper rolling simulation.

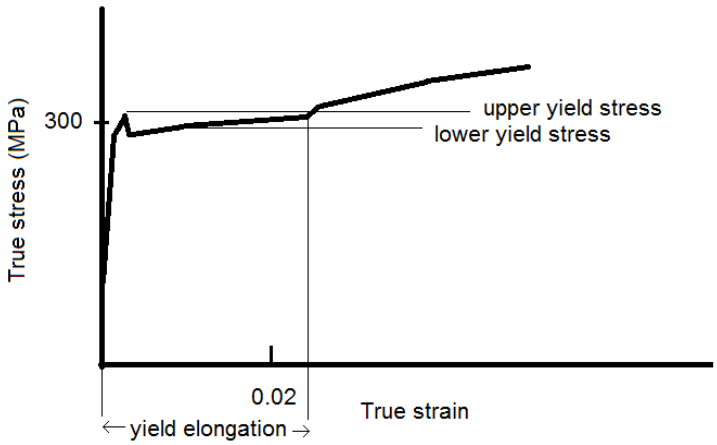

Figure 1 – Typical flow curve for annealed steels (adapted from Wiklund et al., 2002).

Some authors state that in a reduction of a thin and hard strip appears a "plastic contained region" where the plastic deformation of the strip does not occur, due to a three axial compression stress state, and the roll flattens (Johnson and Fleck, 1987, 1992 ; Domanti et al., 1994; Kainz et al., 2003; Shigaki et al., 2015). Example of this flattening effect of the roll can be seen in Figure 2. Others disagree on the existence of this flat region (Liu and Lee, 2001; Chandra and Dixit, 2004), where there is no change in the thickness. These models also assume the hypothesis that the changing of the stresses along the thickness of the strip is negligible, although others (Du et al., 2010) disagree and show that not neglecting it the model produces more consistent results than those other ones. In fact, in that region takes place a very complex stress state, where the direction of the interfacial shear stress changes, the normal pressure is the highest possible, and there are front and back tensions. Besides that, the behavior of the coefficient of friction is not totally understood inside the arc of the contact. It is known that the plastic deformation in these extreme situations happens in two regions in the roll bite: first in the beginning and the other after the plastic contained region.

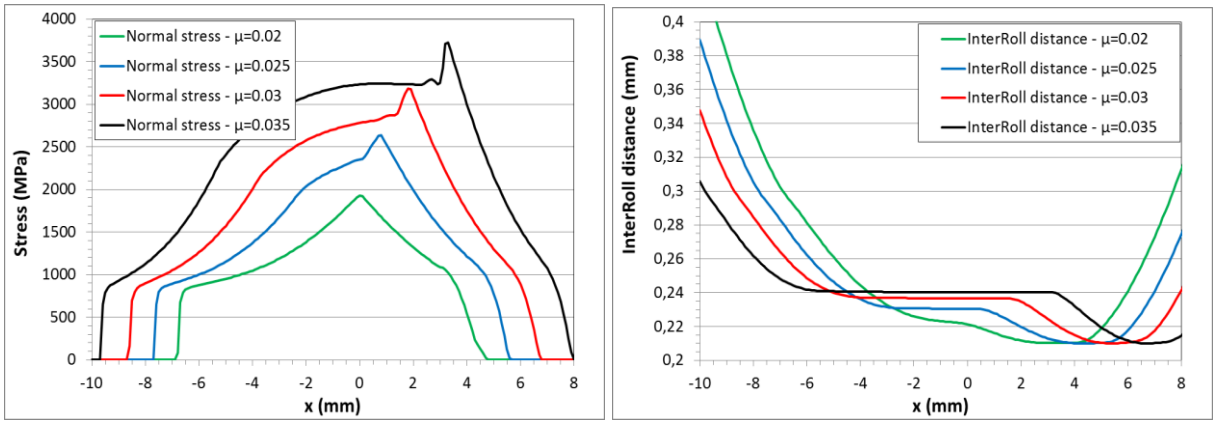

Figure 2 – Normal stresses inside the contact arc (left figure) and the roll deformation profile (right figure) for four different friction coefficients. Note the flattened region of the roll (Shigaki et al., 2015).

Unfortunately, those mathematical models for hard and thin strips based on the slab method fail when applied to temper rolling process for many conditions. One of the reasons is that the initial contact length is very low, and it produces a peak on the normal pressure that

deforms excessively the roll, making the program to be very hard to converge, unless some "tricks" are applied: high relaxation on the profile and pressure change from one iteration to another, growing slowly the yield strength, etc…

Related to the radial deformation of the roll, Krimpelstaetter and co-workers (2005) presented a skin pass model in order to calculate rolling forces and torques for very thin and hard strips including the roll's deformation in the circunferential sense. They showed the importance to take this deformation into account for high friction cases and thin strips.

Different researchers developed the modeling of the temper rolling process with the finite element method. Gratacos et al. (1992, 1994) developed a full FE – strip and roll, elstic-plastic - model in plane strain, as simpler models cannot predict the parameters for temper process. But even with a more precise model, the lack of sliding velocity evaluations for the strip/roll interface and, at that time, computational time, were some of the difficulties. Simplifying assumptions on the behavior of the material as a rigid-plastic one (see, e.g. Chandra and Dixit, 2004) or adopting rigid rolls should not be used for the temper rolling simulation for the aforementioned reasons.

There is a lack of experimental data to validate models for temper rolling process, though the work by Sutcliffe and Rayner (1998) should be mentioned. In their work, a plasticine strip and elastomer rolls are used and they showed the existence of the flat region that the model due to Fleck and Johnson states, though the magnitude of the rolling loads were quite different.

Du et al. (2010), developed a model that calculates the correct rolling load taking into account the inhomogeneous distribution of internal stress in thickness direction and lateral flow and they conclude that it was important to give precise values for the rolling loads. Simpler mathematical models assume a homogeneous deformation of the strip, but it is known that it is not true, and only some portions of the strip of the metal deform sufficiently to enter the plastic range (Lenard, 2014). Wang et al. (2005) show that this assumption gives lower rolling loads than industrial measured loads for hot temper rolling process.

Another point concerns about the influence of the strain rate on the results of the temper rolling models. Roberts, in his model, uses a fixed value for a variable named a which represents the change in yield strength per decades of change of the strain rate. Mazur (2012) enforces the importance to take this factor into consideration on the calculations.

Figure 3 shows the flow curves for different strain rates. For low reductions it can be noted high variations on the yield stress according with the strain rate used in the tension test.

It can be seen so far that there is a need for better understanding the temper rolling process in order to achieve better understanding of the rolling mill and achieve a perfect control over it. The finite element method is the most indicated for this task, as less simplifying hypotheses are assumed to calculate the rolling loads, contact arc profile, friction stresses and elastic/plastic stress/strain distribution inside the strip.

The present study develops a finite element model of the temper rolling process, assuming plane strain state. Two cases are analysed. The first case was used to develop the FE nodel and to validate it, based on the paper by Kainz et al., (2003) and on a paper by Gratacos et al. (1992) used as a base model for changes in other parameters in order to analyse the behavior of the temper process. At last, the third case is based on industrial data.

The finite element software Abaqus 16.4.2 were used in this work.

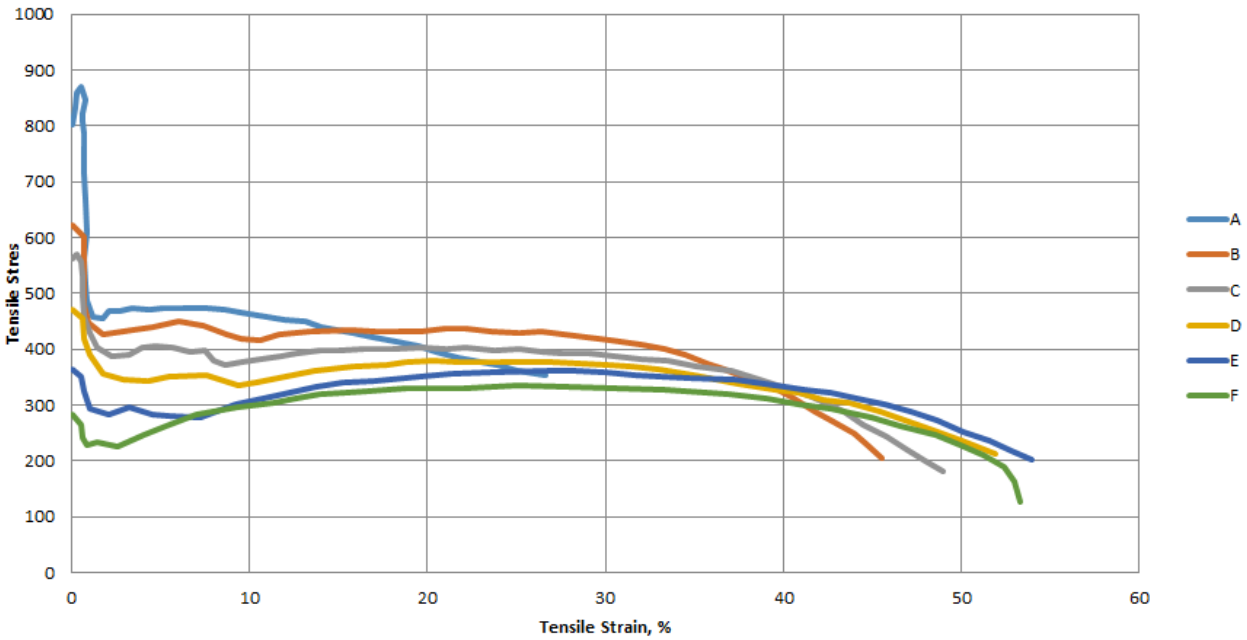

Figure 3 – Flow curves (MPa x % strain) for a low carbon steel and different strain rates (A: 1750 s^{-1}; B: 106 s^{-1}; C: 55 s^{-1}; D: 10 s^{-1}; e: 2s^{-1}; F: 0.001 s^{-1}) (Adapted from Blazynski, 1987)

2 FINITE ELEMENT MODEL OF THE TEMPER ROLLING PROCESS

The work made by Zeman and co-workers (Zeman et al., 2005) was taken as a reference for developing the FE model and for its validation.

In order to have a deeper understanding of the contact between the work roll and the strip in the temper rolling process, it was modeled an explicit dynamic simulation, using the non-linear capabilities present on Abaqus 6.14.2. It is assumed a 2D plane strain state.

The objective of this FE model was to simulate the temper rolling process. Typical for this process is the low reduction applied on the strip, and its thickness is less than 0.66 mm. To achieve an accurate result, an extremely fine mesh is required on the strip (Figure 4). The medium size of the elements in the contact interface between the strip and the roll must be the same. In our model, this value was 0.025mm.

In order to reduce the problem size and complexity, partitions were made on the work roll to provide a fine to coarse mesh transition, and due to symmetry properties, relative to the horizontal mid-plane, just the upper half of the setup was modeled.

The convergence was tracked controlling the kinectic energy along the step. It was observed that for a time step of between 8 to 9ms was enough to give more contant results.

Two major steps were used. Tha first for the rolling process itself, and the second for relieving the strip from rolling load and front and back tensions.

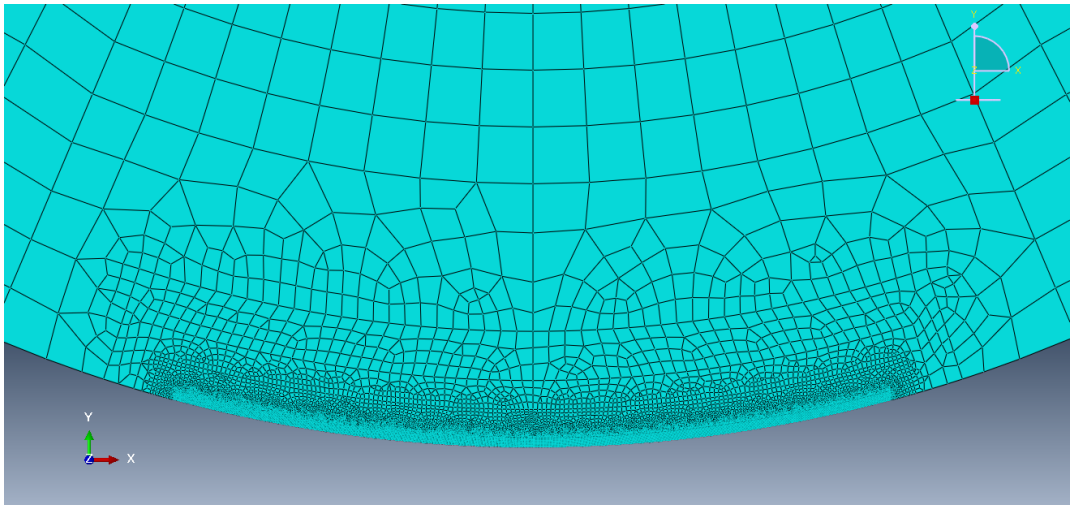

Figure 4 - Fine to coarse mesh transition on the work roll.

The inner ring was modeled as a rigid body driven by a constant velocity on the reference point in the work roll center. This kind of simplification does not affect the work roll deformation as long as the rigid body radius remains small compared to the outer work roll radius and due to Saint Venant principle.

The initial conditions computed on the model were an angular velocity applied on the reference point of the work roll center, and the second condition was an initial linear velocity on the x direction on the strip. The initial strip velocity was chosen to match the linear velocity on the outer radius of the work roll.

The boundary conditions imposed on the work roll reference point were a constant angular velocity, and a restriction on x and y coordinates allowing just the rotation about the z axis. The strip boundary conditions were a back tension, a front tension, and a symmetry condition on plane xz, so that only the upper half of the mill was modeled (see Figure 5).

The contact model used between the work roll and the strip was the surface-to-surface interaction using the mechanical constraint formulation based on the kinematic contact method. The details are: Contact property options: Tangential behavior; Friction formulation: Penalty; Directionality of friction: isotropic; Friction coefficient: μ; Mechanical constraint formulation: kinematic contact method; Sliding formulation: finite sliding; Weighting factor: use analysis default

The region that first enter in contact with the roll needed to be “rounded” (see Figure 6). This procedure turned the entering process more smooth, with less distortion of the finite elements in that region.

Another modeling detail is the better value for the mass scaling value. This numerical trick accelerates the processing time for explicit dynamic simulations. The higher this value, the higher the processing time, but the stability of the convergence must be tracked. Kainz (Kainz et al., 200) shows that a mass scaling value of 100 gives the best trade off result. But in our model, using a mass scaling of 100 resulted in instability. The processing time was longer, but more precise and stable.

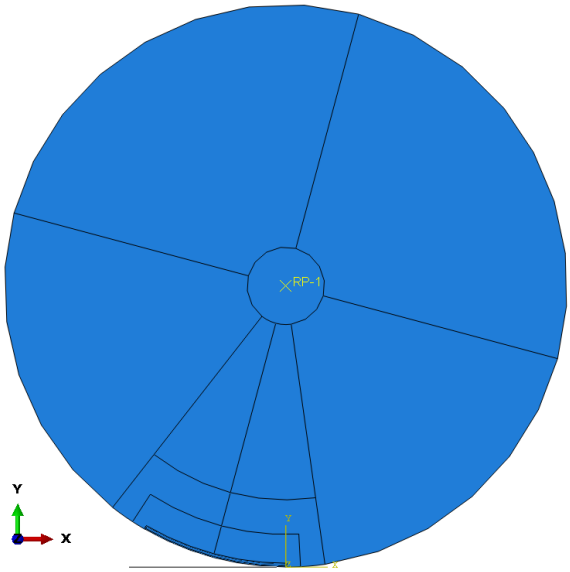

Figure 5 – Roll and strip geometry, including the cutting lines for a good meshing.

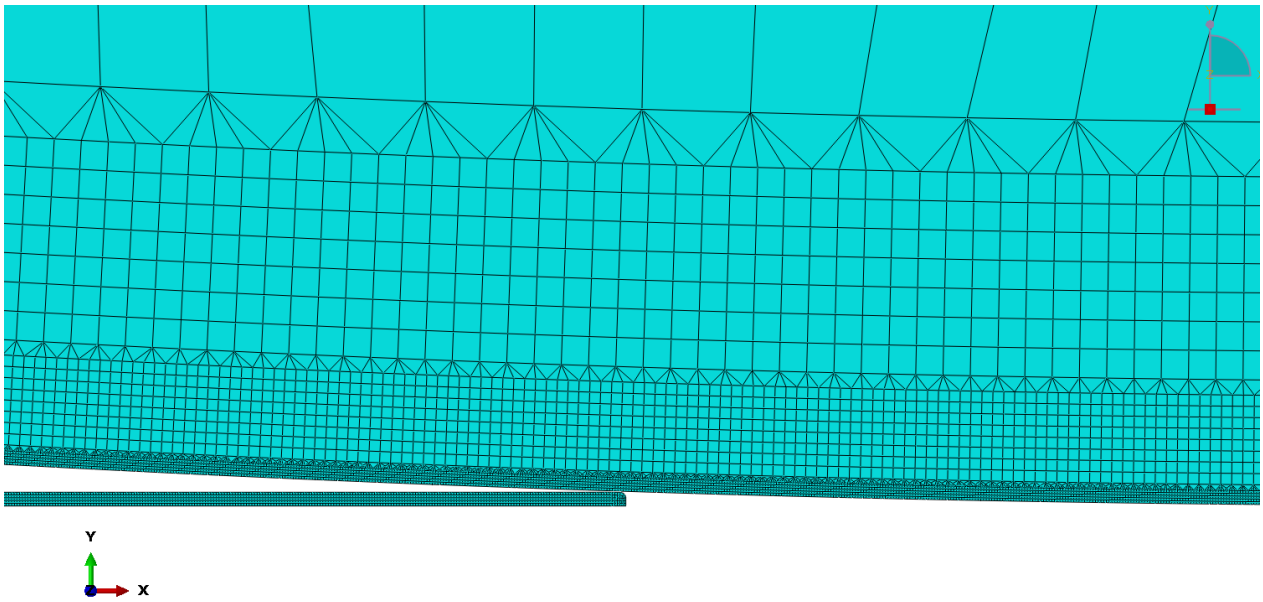

Figure 6 – Detail of the mesh. Note that the strip is "rounded" in the first region that will come into contact with the roll.

The Abaqus/Explicit precision used was doubled – analysis and package, and nodal moutput precision doubled. Otherwise the deformation of the roll was distorted.

As was mentioned above, the temper rolling process is dependent on the strain rate effect over the flow rule at initial deformation. So it was used the Johnson-Cook model for the characterization of the strip's material for the second case.

3 CASES FOR SIMULATION

Two cases were chosen in this study. The first one, a study by Gratacos et al., (1992), they modeled the temper rolling process in 2D via FE explicit method, and presented some results. This was used in order to develop our temper rolling model and calculate results for other operational conditions. The second case is a real one from a major brazilian rolling company. Input data are summarized in the Table 1.

Table 1 – Parameters for Case 1 and 2.

Parameters	Case 1	Case 2
Sheet thickness at entry (mm)	0.660	0.252
Sheet thickness at exit (mm)	0.644	0.250
Work roll diameter (mm)	600	500
Material related coefficient *A* (MPa)	400	290
Material related coefficient *B* (MPa)	20	500
Material related coefficient *n*	1	0.22
Coefficient m (Johnson-Cook)	0	0.5
Material Young's modulus (GPa)	210	200
Working roll Young's modulus (GPa)	210	210
Material Poisson's coefficient	0.3	0.3
Work roll Poisson's coefficient	0.3	0.3
Friction coefficient	0.15, 0.20, 0.25	0.4
Front applied tension (MPa)	37	110
Back applied tension (MPa)	20	25
Rolling speed (m/min)	407.3	650

4 RESULTS

After modeling the temper rolling mill studied in Gratacos et al., 1992, its results were compared with those from our model, giving the same values. Once validated, we started varying other parameters. The results are presented in the following figures.

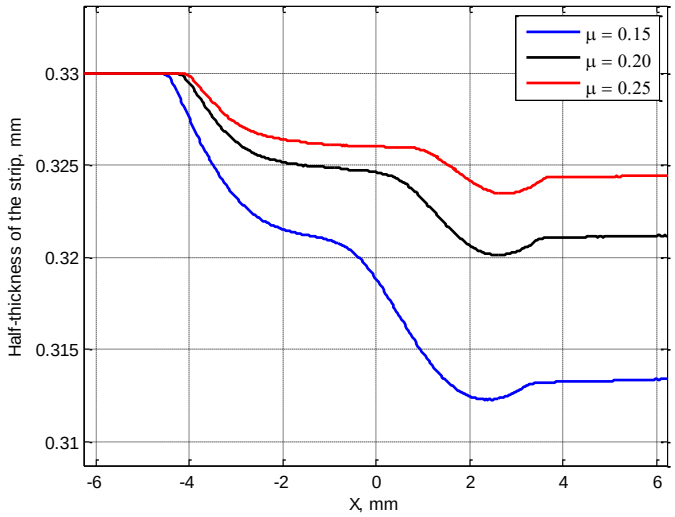

Figure 7 – Half-thickness of the strip for different values of the friction coefficient.

In the Figure 7 the final thickness is higher when the friction coefficient increases.

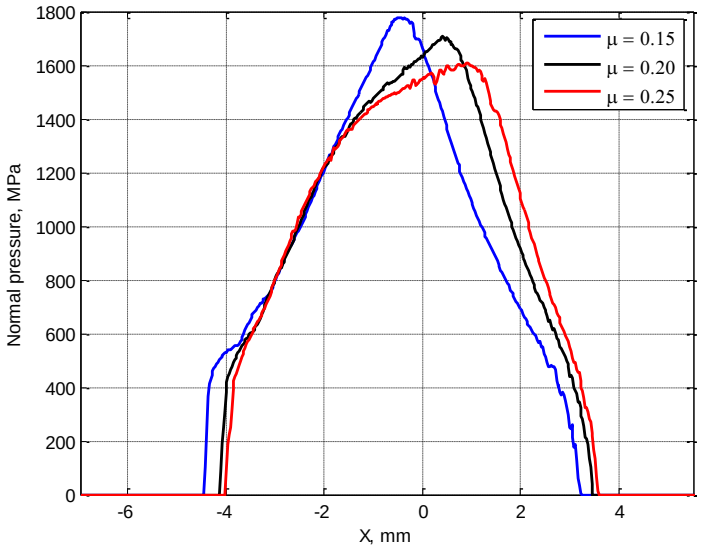

Figure 8– Normal pressure on the strip for different values of the friction coefficient.

In the Figure 8 it can be seen the normal pressures for three different values of coefficient of friction.

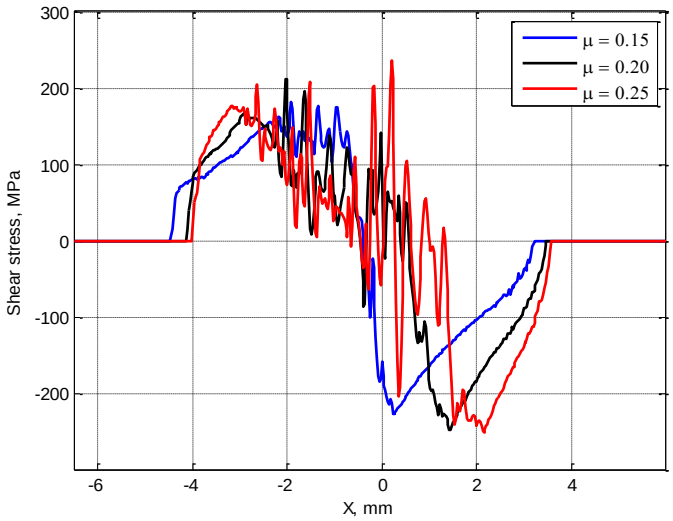

Figure 9 – Shear stress in the interface between the strip and the roll for different values of the friction coefficient.

In the Figure 9 shear stress in the arc of contact is shown. We see clearly the change in the sign of the stress.

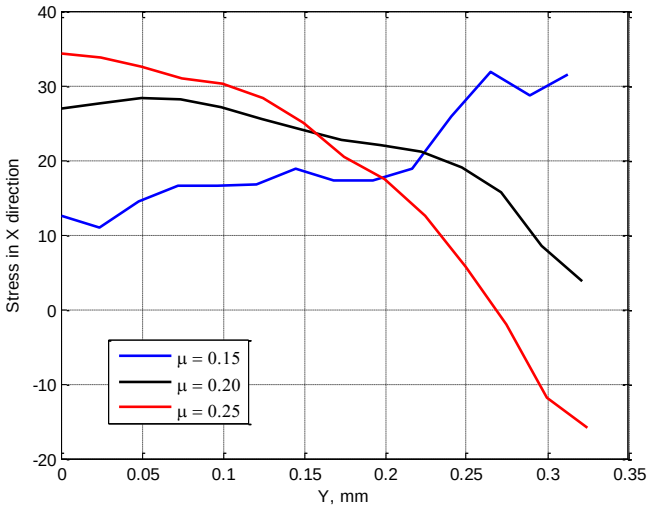

Figure 10 – Stress values in x direction along the half-thickness of the strip, for different values of the friction coefficient.

In the Figure 10 it can be seen the stress in the rolling direction along the thickness of the strip. The difference between the values of the stress in the center of the strip (Y=0) and the stress at the surface of the strip (Y=0.322) increases as long as the friction coefficient increases.

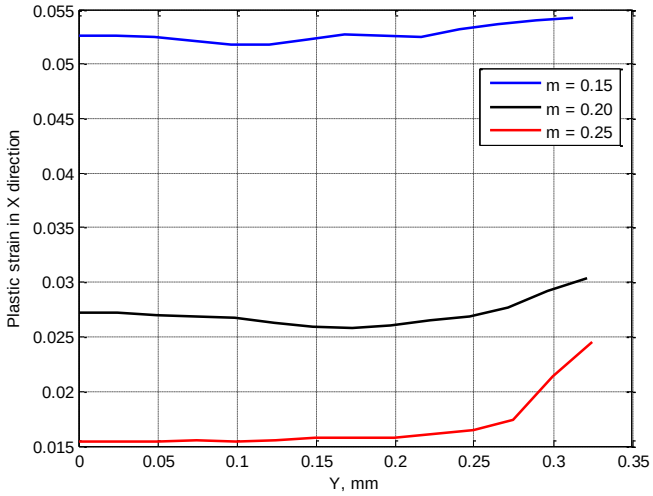

Figure 11 – Plastic strain in x direction along the half-thickness of the strip, for different values of the friction coefficient.

In the Figure 11 the plastic strain is showed along the thickness for three coefficients of friction. Interesting to note that the variation of this stress near the surface increases as long as the coefficient of friction increases.

The following results are for the highest value of μ.

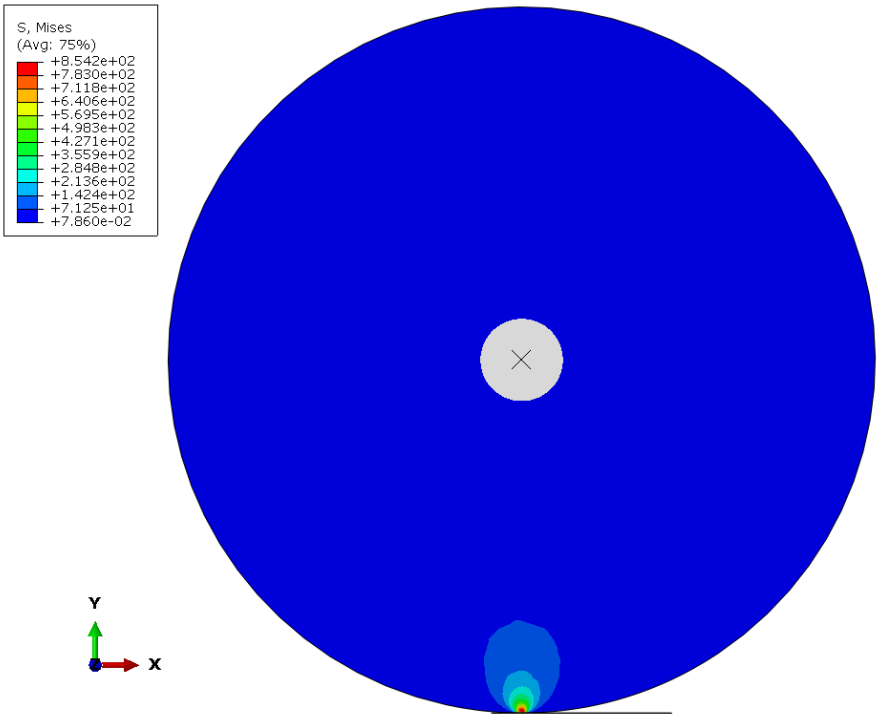

Figure 12 – Von Mises stress.

In the Figure 12 it can be seen the von Mises stress for the roll and strip.

Figure 13 – Von Mises stress in the arc of contact of the strip.

In the Figure 13 von Mises stress for the arc of contact in the strip is shown.

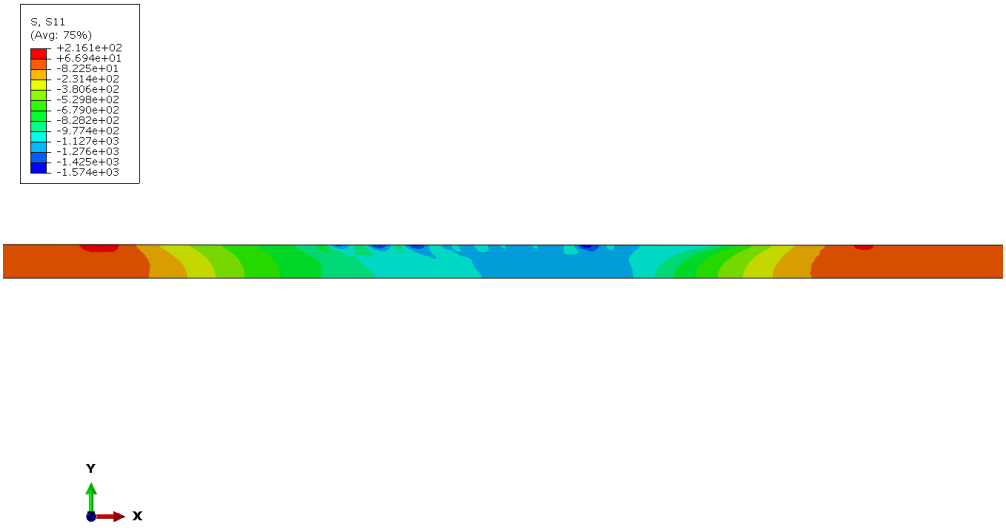

Figure 14 – S11 stress in the arc of contact.

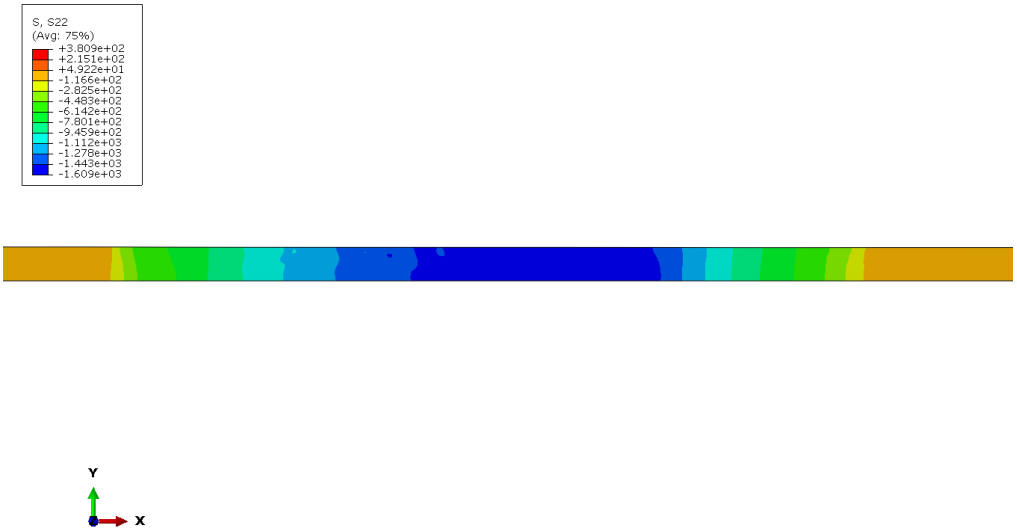

Figure 15 – S22 stress in the arc of contact.

Figure 16 – S33 stress in the arc of contact.

From Figs. 14, 15 and 16 it is noticed that there are compression stresses inside the arc of contact.

The case 2 is an industrial temper rolling mill one from a major brazilian flat rolling company, and its finite element modeling was done to check how close our model is to reality.

Before presenting the results from this simulation, some observations must be made. Unfortunately not all information was given, especially the roll gap, the value of the friction coefficient, and the experimental detailed flow rule of the rolled strip. The thickness of the exiting strip is almost the same of the entering strip, as the precision of the ultrasonic gauge reader reads only 3 floating points and the reduction was very low.

Another point that must be mentioned is that the temper rolling mill train has two 4-high rolling mills in tandem. The experiment was done suddenly stopping in the middle of a

campaign, in order to have the strips the nearest possible from a steady state production. As the stopping does not happen immediately, this fact may have interfered on the readings (for instance, low speed of the rolls means higher friction).

In the Figure 17 normal stresses for Case 2 are shown. We applied two different conditions on Case 2 for the following reason. The total rolling load experimentally measured was 11MN, a value extremely high for a temper rolling process of an annealed low carbon steel… In an attempt to reach that high value for the rolling load, 10 different conditions were tried, varying the friction coefficient, the roll gap and the yielding stress, without success. The Figures 17, 18 and 19 have results for only two cases, being one of them the extreme one (roll gap of 0.002mm and a friction coefficient of 0.60). The maximum value attained for the total rolling load was 7.2MN.

It was observed that the roll can't deform the strip beyond than that (Figure 18).

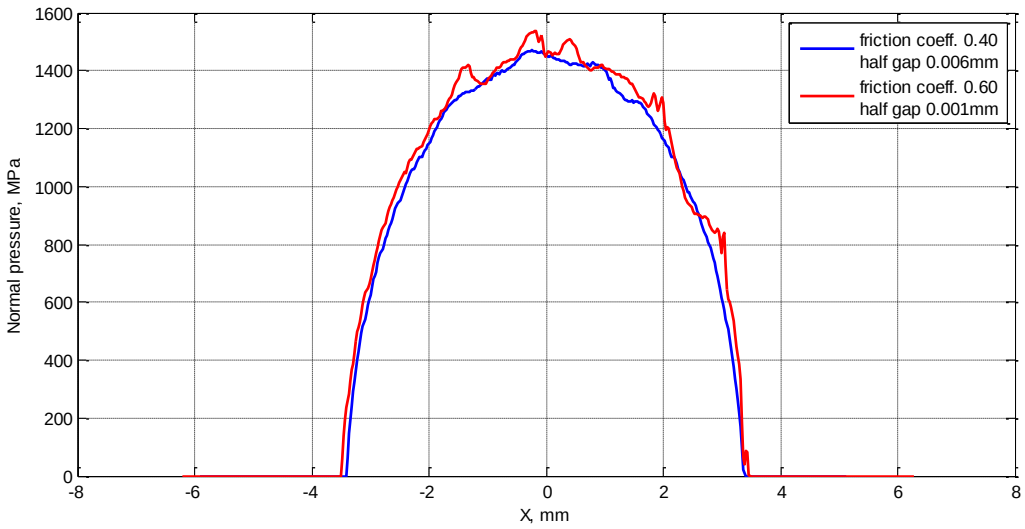

Figure 17 – Normal stress for Case 2 with 2 different conditions.

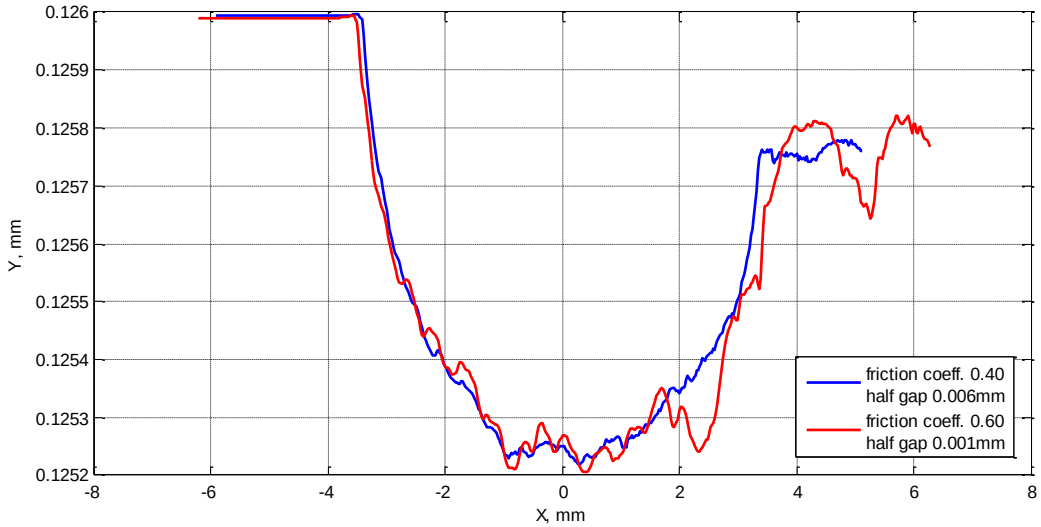

Figure 18 – Profile of the arc of contact for Case 2 with 2 different conditions.

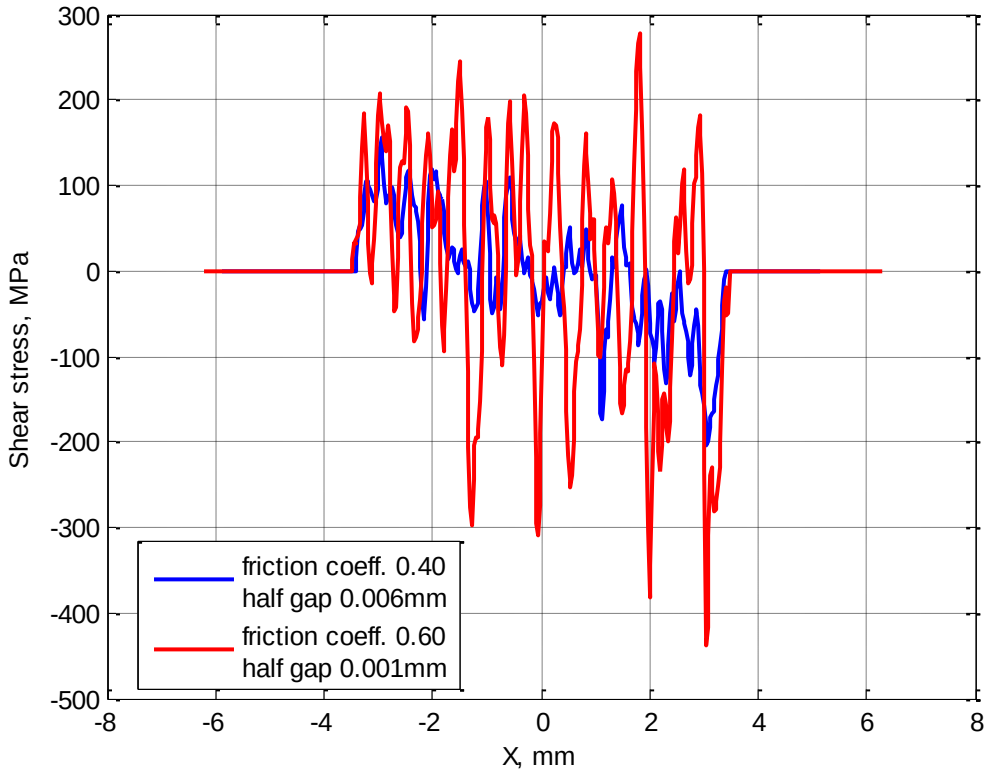

Figure 19 – Shear stress in the interface strip/roll for Case 2 with 2 different conditions.

5 CONCLUSIONS

The temper rolling process was successfully developed with an elastoplastic FE dynamic explicit scheme with Abaqus. Once validated the process of building the FE model, we extrated many results to show the behavior of the temper process on the final product.

In Figure 7 it can be seen that for higher friction values, the output also thickness increases. This is not the usual behavior for flat rolling of strips. It was observed that in temper rolling the rolls deform instead of the strip after some plastic deformation. It can be seen also the flattening at the center of the arc of contact for the highest μ. Integration of the normal pressure curves of Figure 8 shows that the highest coefficient of friction gives the highest total rolling load and that the neutral point goes to the right for higher values of μ.

In Figure 9 it can be seen that when μ increases, the peaks of shear stresses walks away from the center in direction to the entrance and exit of the arc of contact.

In Figure 10 the internal stresses aren't homogeneous, showing a tendency to have tensile stresses on the surface of the strip and compressive stress in the middle, as states Mazur (2012). In Figure 11 it can be seen that near the surface we have higher variation of the plastic strain along the thickness of the temper rolled strip.

In Figure 12 it can be seen the concentrated atress over the contact region, remembering a hertzian shape for von Mises stress distribution on the roll.

From Figs. 13 to 16 the stresses inside the strip in the contact region is shown. The highest values of Mises stresses occur in the roll gap. A triaxial compression stress state is observed on the Figs. 14, 15 and 16. This complex state helps to prevent plastic deformation in part of that region.

From the results obtained for Case 2 it was stated that the value of the total rolling load calculated by the FE model is much less than the measured one (7.2/11 = 65% of the measured load). One serious doubt is that the material of the strip is soft (low carbon steel) and annealed, so that the load should not be so high… But for the reasons already presented on the experimental procedure and the lack of more information, we need more experiments to take a better conclusion. The fact is that even for the most stringent situation, the roll deforms, and the thickness of the strip does not change in a measurable way. From Figure 18 it can be seen that the entering thickness is 0.126mm (half thickness due to symmetry) and the exit thickness is 0.12575mm.

Many of the facts mentioned in the Introduction were shown here to be true. This research will go on with more experimental data in order to have a better understanding of the temper rolling process. The goal is to improve our knowledge of the process to have better control over it and produce strips with the highest quality, as demands the market.

ACKNOWLEDGEMENTS

We wish to thank CNPq, Proc. 488027/2013-6 and CEFET-MG (Propesq), and CEFET-MG for financial support for participating at Cilamce 2016.

REFERENCES

Blazynski, T. Z. ed. Materials at high strain rates, Elsevier Applied Science, 1987.

Chandra, S., & Dixit, U. S., 2004. A rigid-plastic finite element analysis of temper rolling process. *Journal of Materials Processing Technology*, *152*(1), 9-16.

Dbouk, T., Montmitonnet, P., Suzuki, N., Takahama, Y., Legrand, N., Ngo, T., & Matsumoto, H., 2013, June. Advanced roll bite models for cold and temper rolling processes. In *Proc. 9th Int. Rolling Conf. & 6th European Rolling Conf., Venice, Italy*.

Domanti, S. A., Edwards, W. J., Thomas, P. J., & Chefneux, I. L., 1994, June. Application of foil rolling models to thin steel strip and temper rolling. In *Sixth International Rolling Conference, Dussedorf* (p. 422).

Du, X. Z., Jiang, Z. Y., Bai, Z. H., Yu, X. L., & Zhang, Z. Y., 2010. A new calculating model of rolling pressure during temper rolling process. In *Key Engineering Materials* (Vol. 443, pp. 39-44). Trans Tech Publications.

Fang, X., Fan, Z., Ralph, B., Evans, P., & Underhill, R., 2002. Effect of temper rolling on tensile properties of C-Mn steels. *Materials science and technology*, *18*(3), 285-288.

Fleck, N. A., & Johnson, K. L., 1987. Towards a new theory of cold rolling thin foil. *International journal of mechanical sciences*, *29*(7), 507-524.

Fleck, N.A., Johnson, K.L., Mear, M.E. and Zhang, L.C., 1992, "Cold Rolling of Foil", roc. I. Mech. E., 206, 119–131.

Gratacos, P., & Onno, F., 1994, June. Elastoplastic models for cold rolling, application to temper rolling. In *METEC Congress 94. 2 nd European Continuous Casting Conference. 6 th International Rolling Conference.* (Vol. 2, pp. 441-445).

Gratacos, P., Montmitonnet, P., Fromholz, C., & Chenot, J. L., 1992. A plane-strain elastoplastic finite-element model for cold rolling of thin strip.*International journal of mechanical sciences*, *34*(3), 195-210.

Kainz, A., Krimpelstätter, K., & Zeman, K., 2003, November. FE-simulation of thin strip and temper rolling processes. In *ABAQUS Austria User's Conference*.

Lenard, J. G. (2014). *Primer on flat rolling*. 2nd ed. Elsevier.

LIU, Y., & LEE, W. H., 2001. Application of the preliminary displacement principle to the temper rolling model. *KSME international journal*, *15*(2), 225-231.

Pawelski, H., 2000. Modelling of temper rolling considering surface change of strip. In *8 th International Conference on Metal Forming* (pp. 285-293).

Roberts, W. L. (1988). *Flat rolling of steel*. Dekker.

Shigaki, Y., Nakhoul, R., & Montmitonnet, P., 2015. Numerical Treatments of Slipping/No-Slip Zones in Cold Rolling of Thin Sheets with Heavy Roll Deformation. *Lubricants*, *3*(2), 113-131.

Sun, J. N., Huang, H. G., Du, F. S., & Li, X. T., 2009. Nonlinear finite element analysis of thin strip temper rolling process. *Journal of Iron and Steel Research, International*, *16*(4), 27-32.

Sutcliffe, M. P. F., & Rayner, P. J., 1998. Experimental measurements of load and strip profile in thin strip rolling. *International journal of mechanical sciences*, *40*(9), 887-899.

Wang, L. P., Lian, J. C., Wu, X. D. & Jia, X. (2005) A new rolling force model for dry thick temper rolling strip mill. *Journal of materials processing technology*, 170, 381-384.

Wiklund, O. L. O. F., Sandberg, F. R. E. D. R. I. K., & Lenard, J. G., 2002. Modelling and control of temper rolling and skin pass rolling. *Metal Forming Science and Practice, Elsevier Science Ltd., Oxford*, 313-343.

Zeman, K., Krimpelstaetter, K., Kainz, A., Finstermann, G., Glanner, G., & Paesold, D., 2005. Consideration of Circumferential Work Roll Surface Displacements in a Non-circular Arc Temper Rolling Model. In *VIII International Conference on Computational Plasticity, CIMNE, Barcelona, Spain*.